

## Drought Monitoring Using Remote Sensing Data in Nusa Tenggara Timur Province, Indonesia in Between 2018 and 2023

Tati Budi Kusmiyarti<sup>1</sup>, I Wayan Sandi Adnyana<sup>1</sup>, I Wayan Nuarsa<sup>1</sup>,  
I Made Sudarma<sup>1</sup>, I Made Oka Guna Antara<sup>2\*</sup>

<sup>1</sup> Doctor Study Program of Environmental Science, Graduate Program, Universitas Udayana, Jalan P.B. Sudirman, Denpasar, Bali 80232, Indonesia

<sup>2</sup> Research Center for Environmental (PPLH), The Institute of Research and Community Services (LPPM), Universitas Udayana, Jalan P.B. Sudirman, Denpasar, Bali 80234, Indonesia

\* Corresponding author's e-mail: oka@unud.ac.id

### ABSTRACT

This study utilized remote sensing data to monitor the relationship between land cover and drought exposure in Nusa Tenggara Timur (NTT) Province. NTT is a province in Indonesia, located in the Nusa Tenggara archipelago, characterized by low to medium rainfall, which contributes to frequent drought events. In 2018 and 2019, the province was impacted by El Niño, resulting in approximately 865,900 and 1,154,714 affected and displaced individuals, respectively. Due to the limited availability of time-series data, observations from the Landsat-8 OLI/TIRS mission, spanning from 2018 to 2023, were utilized. The normalized difference vegetation index (NDVI) was employed to assess land conditions, while the vegetation health index (VHI), calculated from the Temperature Condition Index (TCI) and vegetation condition index (VCI), was used to estimate drought severity. To validate the dry season period in the study area, ERA5 climate reanalysis data from 1990 to 2020 was used. This study provides new insights into drought monitoring in NTT Province, Indonesia, by analyzing temporal variations in vegetation. The results indicated that seasonal dynamics, climatic variability, seasonal farming practices, and land fires are major contributors to severe drought conditions in NTT. Notably, this research highlighted a finding absent from previous studies: seasonal farming and land fires are the primary drivers of elevated drought levels in the province. The study is significant, as it elucidated the impacts of drought on development, agriculture, and water resources. Through remote sensing data, it revealed spatial drought distribution patterns during the study period in NTT. This research could provide information about land-use and environmental planning in tropical regions.

**Keywords:** remote sensing, drought monitoring, Nusa Tenggara Timur, land cover, vegetation health index.

### INTRODUCTION

Drought is one of the natural disasters with a slow progression. Numerous industries are affected, including agriculture, food security, tourism, health, energy production, and water supply (Al-Kindi et al., 2023; Almouctar et al., 2024; Zeri et al., 2021). While droughts can repeatedly occur in certain regions, each event is unique in terms of its intensity and duration. Because of the geographical and temporal variability brought on by climate change, the relationship between

climate and the frequency as well as recurrence of droughts is still unclear (Abatzoglou et al., 2018; Ghebregabher et al., 2020; Wang et al., 2023).

Monitoring drought conditions is an important and timely effort that is necessary to lessen the effects of both unforeseen and recurring disasters. Combining hydrological and meteorological data allows it to assess the severity, length, and geographic reach of a drought (Li et al., 2021; Liu et al., 2019). Drought duration is closely correlated with its intensity, which is determined by the lack of precipitation (Stanke et al., 2013). When

analyzing the spatial distribution of drought, it is crucial to keep in mind that micro-scale dryness is not always foreseeable and that drought events might occur in different places throughout time (Dai et al., 2018; Li et al., 2021; Liu et al., 2019).

The Republic of Indonesia, located in a tropical region, is significantly impacted by drought events, affecting various sectors across the country, especially in the NTT Province (Kennedy, 2023; Zaki and Noda, 2022). In 2018 and 2019, drought had significant consequences in the province, leading to approximately 865,900 and 1,154,714 people being affected and displaced, respectively (BPS-Statistics Nusa Tenggara Timur Province, 2024a, 2024b; Karuniasa and Pambudi, 2022). However, keeping track of droughts is difficult due to a lack of data. As a result, scientists are now using satellite remote sensing technologies, which are essential for researching the drought-affected regions. These tools enable to track changes in land surfaces, vegetation health, soil moisture, and water availability by examining satellite imagery. Resource allocation, disaster response, and drought mitigation methods are determined by the knowledge gathered from remote sensing (Almouctar et al., 2024; Zeng et al., 2022, 2023). Therefore, the goal of this research was to use remote sensing data to monitor

the relationship between land cover and drought exposure in the NTT Province.

## MATERIAL AND METHODOLOGY

### Study area

The NTT Province ( $8.6574^{\circ}$  S,  $121.0794^{\circ}$  E) located in the Republic of Indonesia's Nusa Tenggara Archipelago, as shown in Figure 1. The NTT Province is home to about 4.3 million people and has an area of about 4.6 million hectares, of which 1.7 million hectares are wooded. The area has shallow, rocky soil and is 72% steep and rough. Less than 2 meters of precipitation fall in the arid regions of NTT each year (Putri et al., 2021). The temperature was  $15.8^{\circ}\text{C}$  (lowest) and  $32.8^{\circ}\text{C}$  (highest) in 2023, while the average temperature was 27 to  $28^{\circ}\text{C}$  (BPS-Statistics Nusa Tenggara Timur Province, 2024c).

### Data and processing method

Drought monitoring in NTT Province was determined using the data from satellite remote sensing. The Landsat 8 OLI/TIRS on dry season in between 2018 to 2023. The dry season in NTT was determined using the ERA5 data from 1990 to

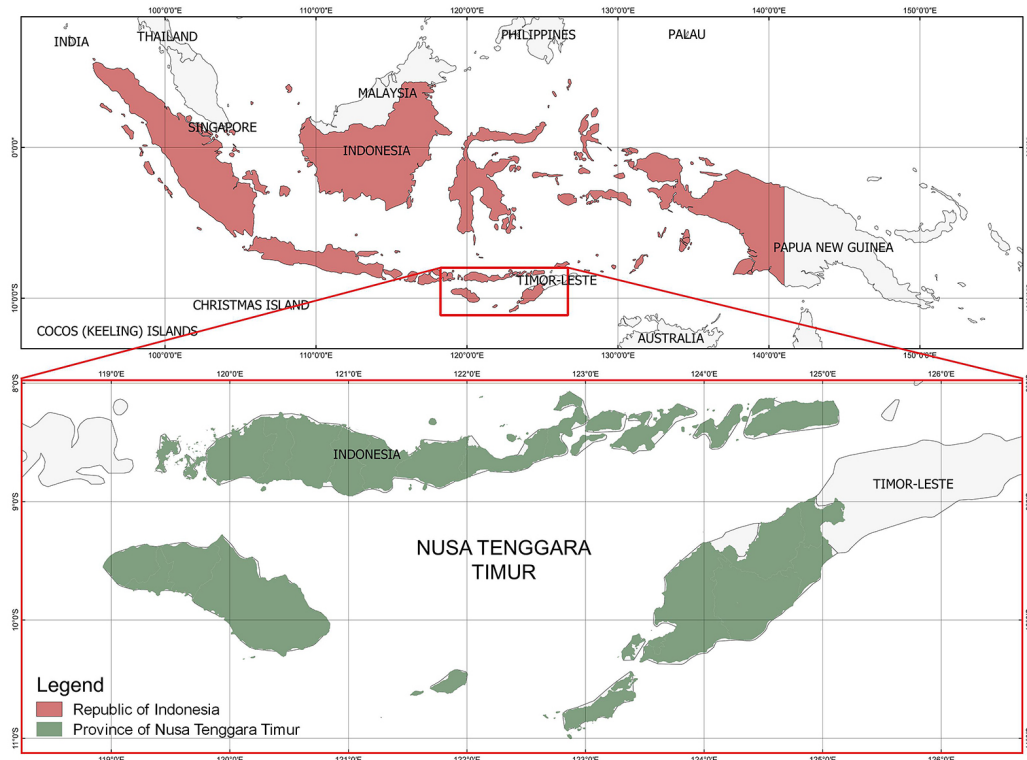


**Figure 1.** Location of study in Nusa Tenggara Timur Province, Republic of Indonesia

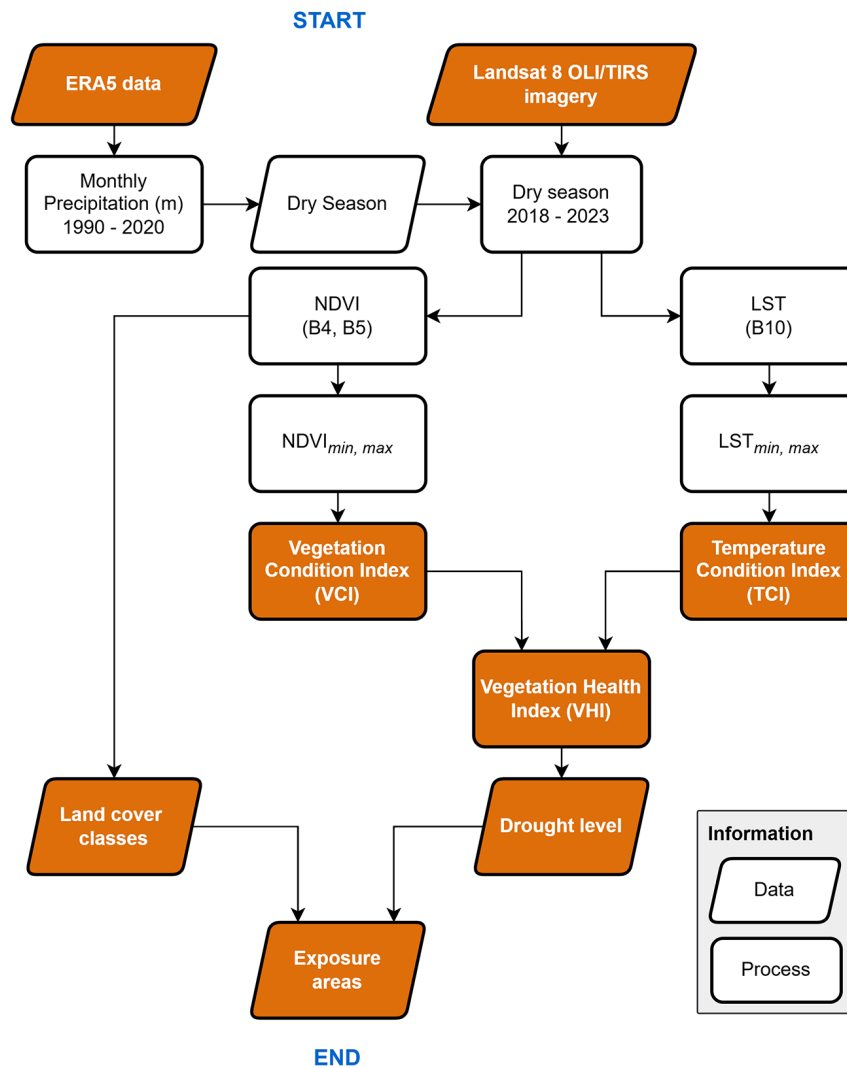
2020. Both of them was accessed and processed through Google Earth Engine platform on URL: <https://code.earthengine.google.com/> (Copernicus Climate Change Service (C3S), 2017; Ermida et al., 2020; U.S. Geological Survey, 2020). The detail of dataset used shown in Table 1. On the other hand, the flowchart of this study is shown in

Figure 2. Landsat 8 OLI/TIRS was used to generate NDVI using Band-4 (B4) for red and Band-5 (B5) for near infrared (NIR) (U.S. Geological Survey, 2020), shown in Equation 1:

$$NDVI = \left( \frac{NIR - Red}{NIR + Red} \right) \quad (1)$$

**Table 1.** Detail of dataset used

No.	Datasets	Variable	Cloud cover	Resolution	Sources
1	Landsat 8 OLI/TIRS (LANDSAT/LC08/C02/T1_L2)	NDVI, LST, VCI, TCI, VHI	10%	10 m median values of Jun to Oct in 2018 to 2023	U.S. Geological Survey downloaded via Google Earth Engine (U.S. Geological Survey, 2020)
2	ERA 5 (ECMWF/ERA5/DAILY)	Precipitation		1990–2020	Copernicus Climate Change Service (C3S) downloaded via Google Earth Engine (Copernicus Climate Change Service (C3S), 2017)



**Figure 2.** Flowchart estimation drought level

NDVI has values ranging from -1.0 to +1.0, normally non-vegetation has values below -0.1, while dense vegetation has values closer to +1.0. The Land Surface Temperature (LST) was generated using a Band-10 (B10) Thermal Infrared Sensor (TIRS) (U.S. Geological Survey, 2020). In the Google Earth Engine platform, the LST value is needed for rescaling, and in conversion to degrees Celcius from Kelvin, as shown in Equation 2:

$$LST = (B10 \times 0.00341802) + (149 - 273.15) \quad (2)$$

The number of 0.00341802 was scaling values, 149 was offset values, and -273.15 was conversion from Kelvin to degree Celsius.

### Precipitation characteristics in between 1990 and 2020 based on the ERA5 data

The average of precipitation characteristics was used to obtain the information about the dry season in NTT by using ERA5 data. ERA5 is the fifth generation of ECMWF reanalysis for the past eight decades of global climate and weather, available from 1940 (Copernicus Climate Change Service (C3S), 2017). The average was generated from 30 years (1990 to 2020), using the average in each month as shown in Figure 3 with red dashed line. Thus, the NTT dry season

**Table 2.** Drought level based on VHI

No.	Drought level	VHI values
1	Extreme	<10
2	Severe	10-20
3	Moderate	20-30
4	Mild	30-40
5	No	>40

was selected from June (5.94 m/month) to October (8.48 m/month).

### Vegetation health index based on Landsat 8 OLI/TIRS

VCI is a percentage that indicates the current values position in relation to the lowest and greatest values recorded in prior years. On a scale of 0 to 100, VCI falls between 0 (very unfavorable) and 100 (great). The values that are closer to zero represent ideal growing circumstances for plants, whilst the values that are closer to one represent the opposite. The formulation of VCI is based on the NDVI values in the present observation,  $NDVI_{min}$  from minimum, and  $NDVI_{max}$  from maximum values of NDVI, shown as Equation 3:

$$VCI = \left( \frac{NDVI - NDVI_{min}}{NDVI_{max} - NDVI_{min}} \right) \times 100 \quad (3)$$

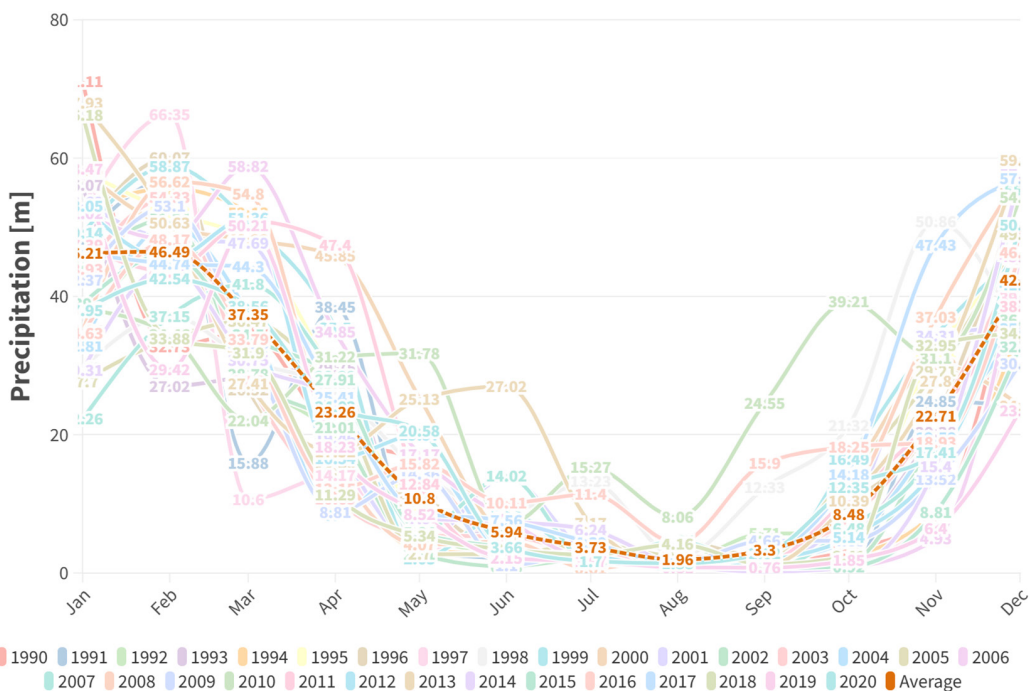


**Figure 3.** Precipitation characteristic in between 1990 and 2020 in Nusa Tenggara Timur Province, Republic of Indonesia

### Temperature condition index based on Landsat 8 OLI/TIRS

TCI is generated from LST values, with values ranging from 0 (very unfavorable) to 100 (great). The TCI formulation is based on LST values in the present observation,  $LST_{min}$  from minimum, and  $LST_{max}$  from maximum values of LST, shown as Equation 4:

$$TCI = \left( \frac{LST - LST_{min}}{LST_{max} - LST_{min}} \right) \times 100 \quad (4)$$

### Vegetation health index

Health of plants is measured by VHI. It is widely used to search for signs of drought using data from satellite remote sensing. VHI was computed using VCI and TCI, with values from 0 to 100%, same as TCI and VC. The extreme drought is indicated by the values close to 0%, and no drought is indicated by the values close to 100% (Table 4). Because it produced good findings using both the TCI and VCI, this index was more comprehensive. The VHI formula, which has a constant ( $\alpha$ ) of 0.5, combines the TCI and VCI formulas, shown as Equation 5:

$$VHI = \alpha \times VCI + (1 - \alpha) \times TCI \quad (5)$$

### Land cover classes based on NDVI

To determine the exposure to drought in the NTT Province region, a land classification was

made based on NDVI values, the classification is shown in Table 3. The value range adopts the range created by (Akbar et al., 2019), consisting of 6 classes, namely water, built-up, barren land, shrub and grassland, sparse, and dense vegetation.

## RESULTS AND DISCUSSION

### Temperature analysis

VHI was computed by using LST and NDVI, the time series of LST observation is shown in Figure 4. However, the LST observation lacks data in some regions on Sumba and Timor Island, this problem occurs only on TIRS/Band-10. The LST value ranged from 11 to 59 °C in 2018, 16 to 61 °C in 2019, 16 to 57 °C in 2020, 5 to 57 °C in 2021, 13 to 62 °C in 2022, and 13 to 62 °C in 2023, based on LST observations.

The high temperature was the effect of El Nino and IOD positive events, except from 2020 to 2022 (Bureau of Meteorology Australia, 2024; NOAA, 2024). There was a land fire in NTT in 2022 and 2023, particularly in Sikka Regency, during Indonesia’s La Nina 2022 (Welianto, 2022, 2023). Therefore, in 2022 LST reached the same value as in 2023. Moreover, zinc predominates on residential roofs in NTT Province. Built-up and barren areas make up the majority of Sumba Island’s land cover. According to (Ogashawara and Bastos, 2012), high temperature has a positive link with that, which leads to the high LST in the NTT province.

The TCI time series findings for NTT Province are displayed in Figure 5. TCI was calculated using the current, minimum, and maximum LST values. As it can be seen in Figure 4, land cover also contributed to TCI. TCI is heavily impacted by land cover changes, which primarily occur in places where there is frequent change, like rice

**Table 3.** Land cover classes on NDVI

No.	Class	NDVI values
1	Water	<0.015
2	Built-up	0.015–0.14
3	Barren land	0.14–0.18
4	Shrub and grassland	0.18–0.27
5	Sparse vegetation	0.27–0.36
6	Dense vegetation	>0.36

**Table 4.** Land cover class based on NDVI

No	Class	2018 (ha)	2019 (ha)	2020 (ha)	2021 (ha)	2022 (ha)	2023 (ha)
1	Water	11,950.16	10,927.08	10,966.50	10,879.51	117,82.57	11,059.78
2	Built-up	425,171.20	374,771.61	253,719.59	326,637.77	203,374.66	253,681.46
3	Barren land	620,716.34	584,905.7	520,823.48	455,479.28	345,642.33	481,215.34
4	Shrub and Grassland	1,716,576.85	1,783,715.39	1,644,434.76	1,531,611.06	1,393,028.71	1,603,974.35
5	Sparse vegetation	1,313,611.54	1,348,837.83	1,436,725.12	1,481,329.02	1,664,876.11	1,549,915.21
6	Dense vegetation	564,590.06	549,458.54	785,946.70	846,679.49	1,033,911.77	752,769.98

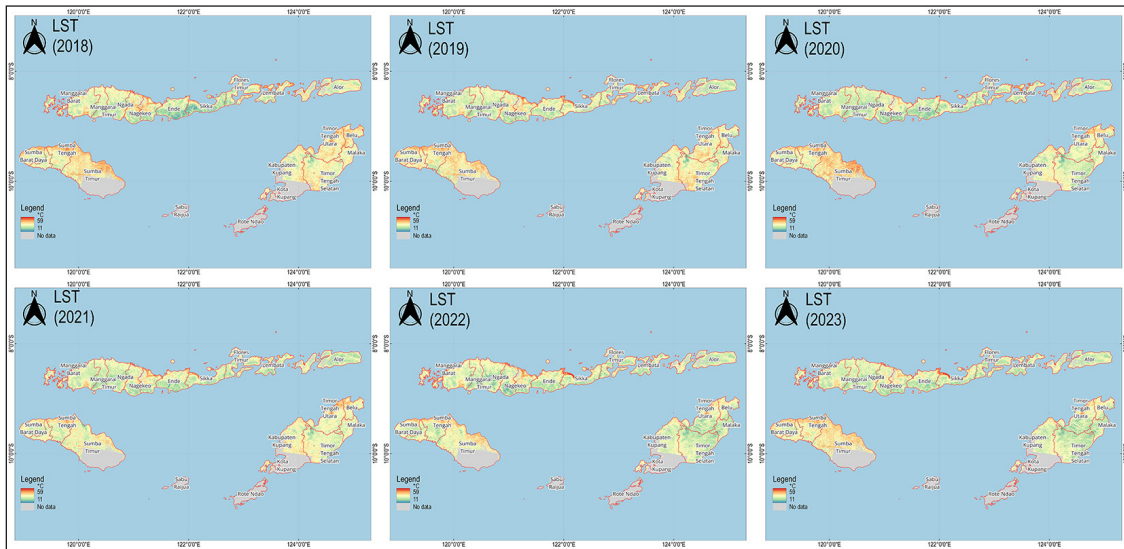


Figure 4. The LST timeseries in NTT Province, Republic of Indonesia in between 2018 and 2023

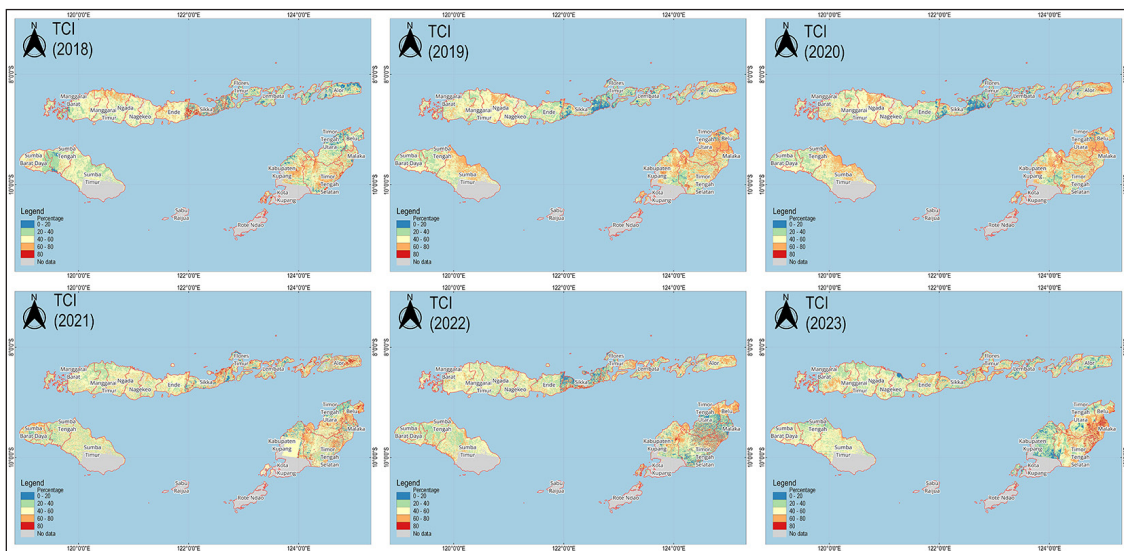


Figure 5. The TCI timeseries in NTT Province, Republic of Indonesia in between 2018 and 2023

fields or other areas used for seasonal farming, as well as impacted by ENSO and IOD.

### Land cover analysis

Land cover was analyzed based on NDVI values following (Akbar et al., 2019), the results of its temporal changes are shown in Figure 6. The figure shows changes in vegetation cover from 2018 to 2023. Table 4 shows the area in hectares for each year and land cover class, while Figure 7 shows a graph of changes in land cover area with reference to the previous year, respectively. In the figure, positive values denote a rise, whereas negative ones denote a drop. Generally, there

is a decrease in the sparse vegetation and dense vegetation classes under the El Nino-affected conditions, while there is an increase under the La Nina-affected conditions. This is inversely proportional to the barren land, shrub and grassland classes. Of course, this is closely related to higher rainfall under the La Nina conditions, so that trees receive more water and also grow better (Diem et al., 2018). Naturally, there is a strong correlation between rainfall and the water class. Consequently, the water rises during La Nina in the NTT province. Eventually, there is a fluctuation in the built-up class; this is brought about by the range of values that are employed as well as additional land cover characteristics that are similar to the class.

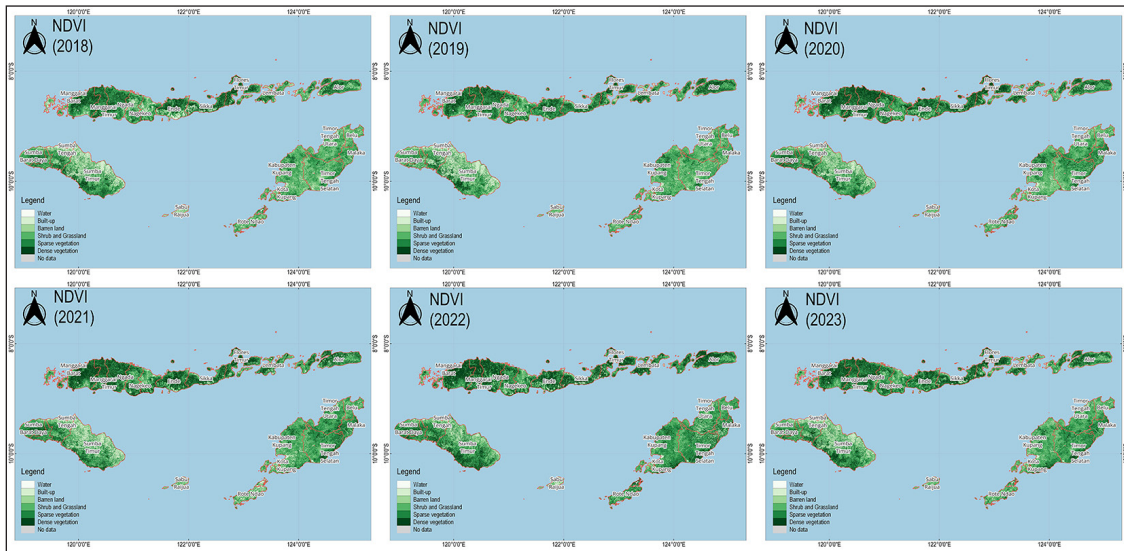


Figure 6. Land cover timeseries in NTT Province, Republic of Indonesia in between 2018 and 2023

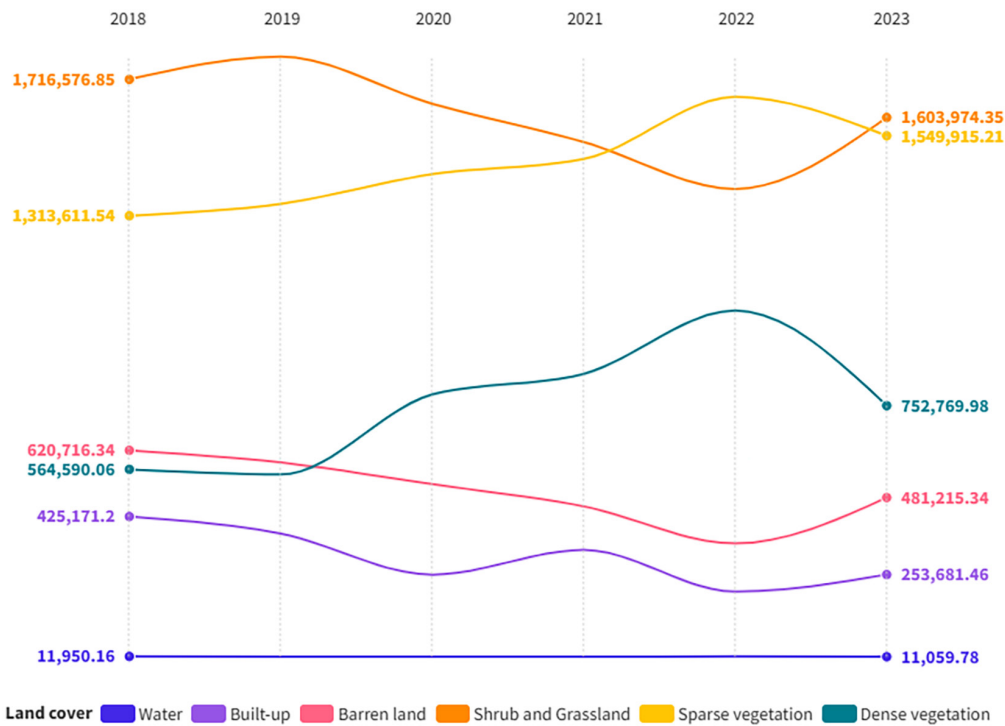


Figure 7. Land cover time series change in NTT Province, Republic of Indonesia in between 2018 and 2023

The VCI time series in NTT was shown in Figure 8. Because the observations were set during Indonesia’s dry season, VCI often has a value of zero. Recurring periods of low VCI readings signify the persistence of drought conditions (Pouyan et al., 2023). While much of the low-topography vegetation has been enduring low circumstances, high-topography vegetation has endured a moderate to severe drought during the research period.

### Areas exposed by drought

The drought indicator for this research was computed by VHI, indicating the regional distribution of drought fluctuations between 2018 and 2023. Table 5 shows the level of drought levels: extreme (< 10%), severe (10–20%), moderate (20–30%), mild (30–40%), and no (> 40%). Figure 7 illustrates the temporal and regional trends of the drought in the NTT Province. It indicates

that a significant portion of the research area experienced no to extreme drought between 2018 and 2023. More than 79% of areas in each period year observed had no drought, less than 0.5% had extreme drought, less than 1.60% had severe drought, less than 6% had moderate drought, and 15% had mild drought, as shown in Table 5.

The graph of increase and decrease of the drought-exposed area is shown in Figure 10. The negative value is decrease and positive value is increase of the drought-exposed area, with reference to the previous year, respectively. Spatially, drought occurs more in the areas with higher population density and agricultural areas, this is caused by land cover change process. Because the analysis process is based on the VHI value, it is related to existing land cover especially vegetation change (Almouctar et al., 2024; Pouyan et al., 2023)(Figure 9).

In contrast to ENSO and IOD, the drought areas during an El Nino event are typically smaller than those during a La Nina event, particularly in the areas with no drought, as shown in Figure 10.

However, in 2022, the largest area experienced extreme drought, which was 17,003.24 ha. That is a rather strange finding, even though at that time the NTT Province experienced the effects of La Nina, as well as being the year with the widest extreme drought area. Most likely, this happened due to land fires in the NTT Province (Welianto, 2022). Then, there was a decline in 2020–2021 for the severe and moderate levels, but an increase in 2022 for the severe level. Ultimately, during periods of mild drought, there was a decline in the exposure to drought until 2022. Regrettably, it climbed again in 2023, almost reaching the level observed in 2018.

The analysis of land cover class exposed by drought level is shown in Figure 11. In 2022, there was an increase in extreme drought exposure in all land cover classes, except water, but it decreased again in 2023. At the severe drought level, barren land, shrub and grassland followed the pattern of the impact of ENSO, where there was an increase in 2019 then decreased and increased from 2021

**Table 5.** Drought level based on VHI

No	Drought level	2018 (ha)	2019 (ha)	2020 (ha)	2021 (ha)	2022 (ha)	2023 (ha)
1	Extreme	3,589.35 (0.09%)	1,354.97 (0.03%)	2,074.92 (0.05%)	1,172.85 (0.03%)	17,003.24 (0.44%)	2,198.84 (0.06%)
2	Severe	34,676.36 (0.90%)	48,520.95 (1.25%)	22,557.80 (0.58%)	18,685.52 (0.48%)	59,753.96 (1.54%)	53,088.67 (1.37%)
3	Moderate	162,888.22 (4.20%)	221,498.89 (5.72%)	106,270.90 (2.74%)	111,332.22 (2.88%)	120,644.55 (3.11%)	202,307.57 (5.22%)
4	Mild	559,277.56 (14.44%)	515,944.99 (13.32%)	542,351.85 (14.00%)	495,757.36 (12.80%)	395,819.72 (10.22%)	549,653.76 (14.19%)
5	No	3,113,383.31 (80.37%)	3,086,112.75 (79.67%)	3,200,125.50 (82.62%)	3,245,404.78 (83.81%)	3,280,786.12 (84.69%)	3,066,870.53 (79.16%)

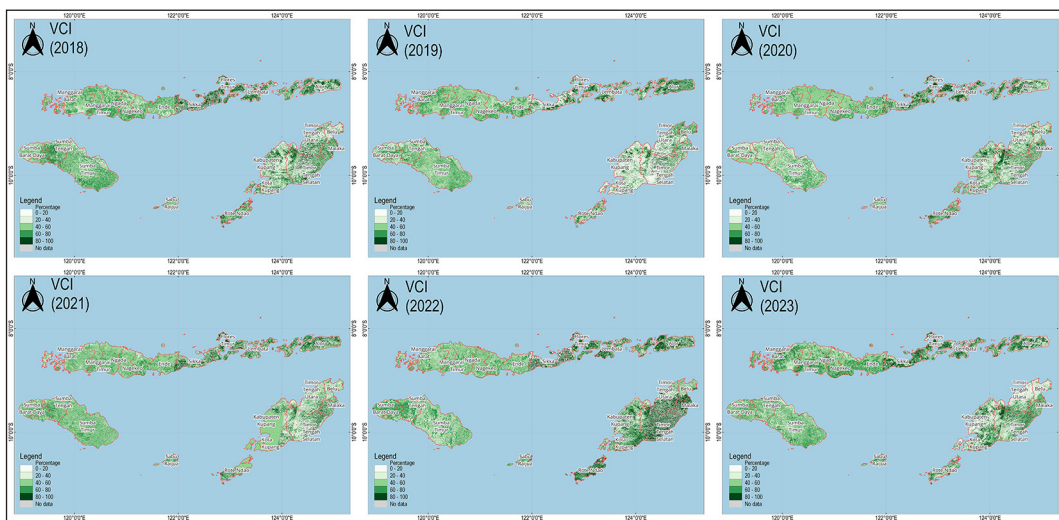


**Figure 8.** The VCI time series in NTT Province, Republic of Indonesia in between 2018 and 2023

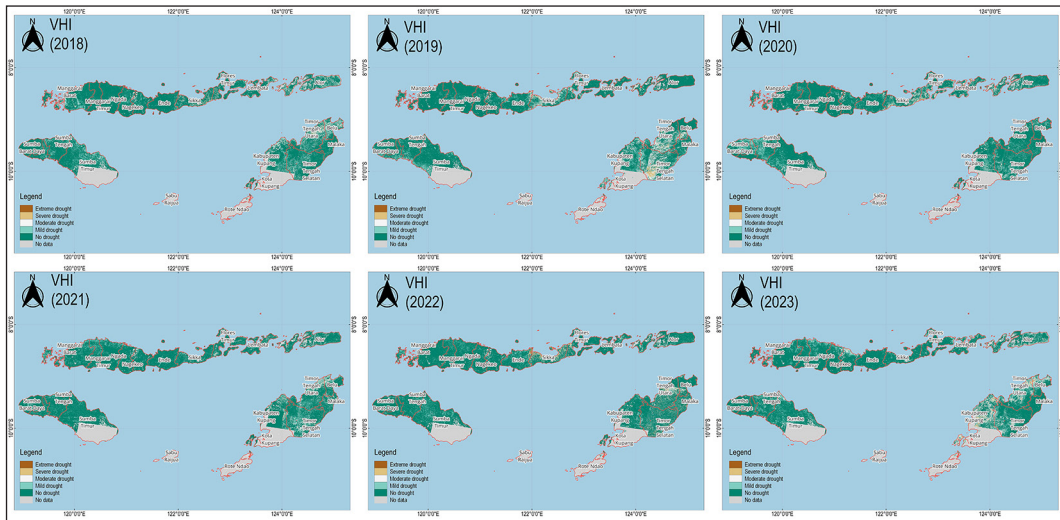


Figure 9. The VHI timeseries in NTT Province, Republic of Indonesia in between 2018 and 2023

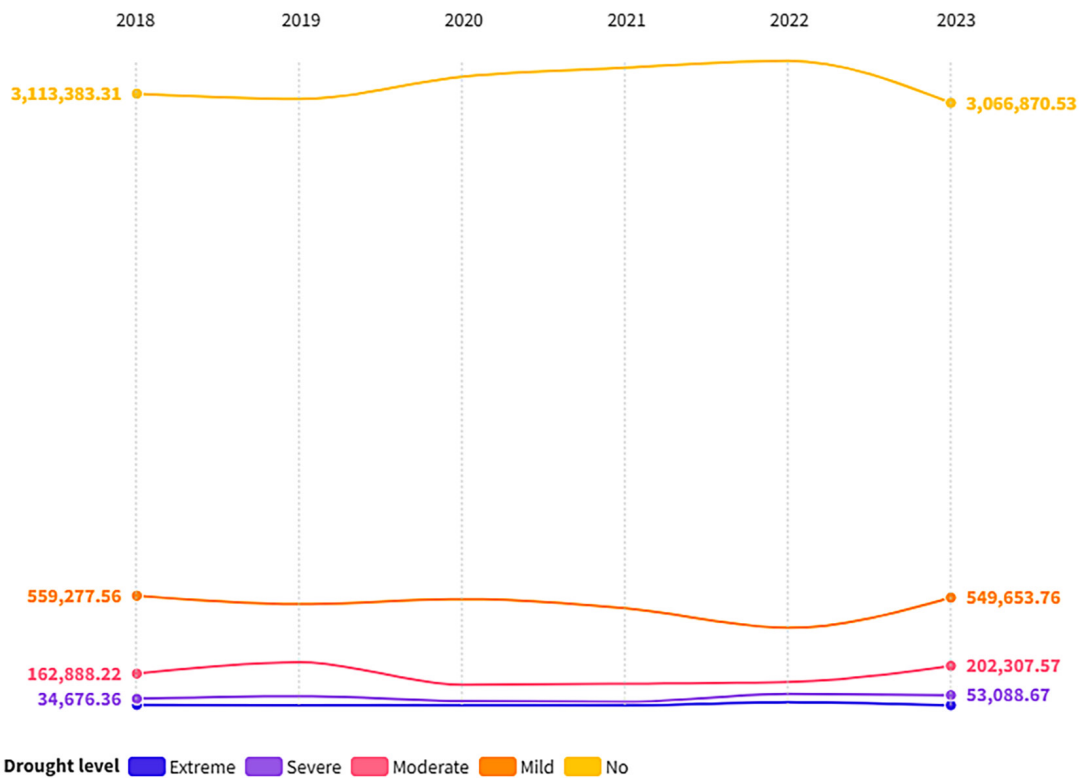


Figure 10. Drought level time series based on VHI in NTT Province, Republic of Indonesia in between 2018 and 2023

to 2023. Meanwhile, sparse and dense vegetation only experienced an increase in drought exposure in 2022, this also happened in the moderate drought class. Finally, at the mild drought level, it was found to be inversely proportional to the severe and moderate classes. When the mild drought level decreased, they increased. Thus, the analysis found that the drought in the NTT

Province was greatly affected by the climate variability of ENSO and IOD, but there was also a relationship with the fire incidents that occurred. Last but not least, the pattern of seasonal plants and their growth related to seasonal variability cannot be excluded in the VHI-based drought analysis process (Almouctar et al., 2024; Nopia et al., 2023; Zeng et al., 2023).

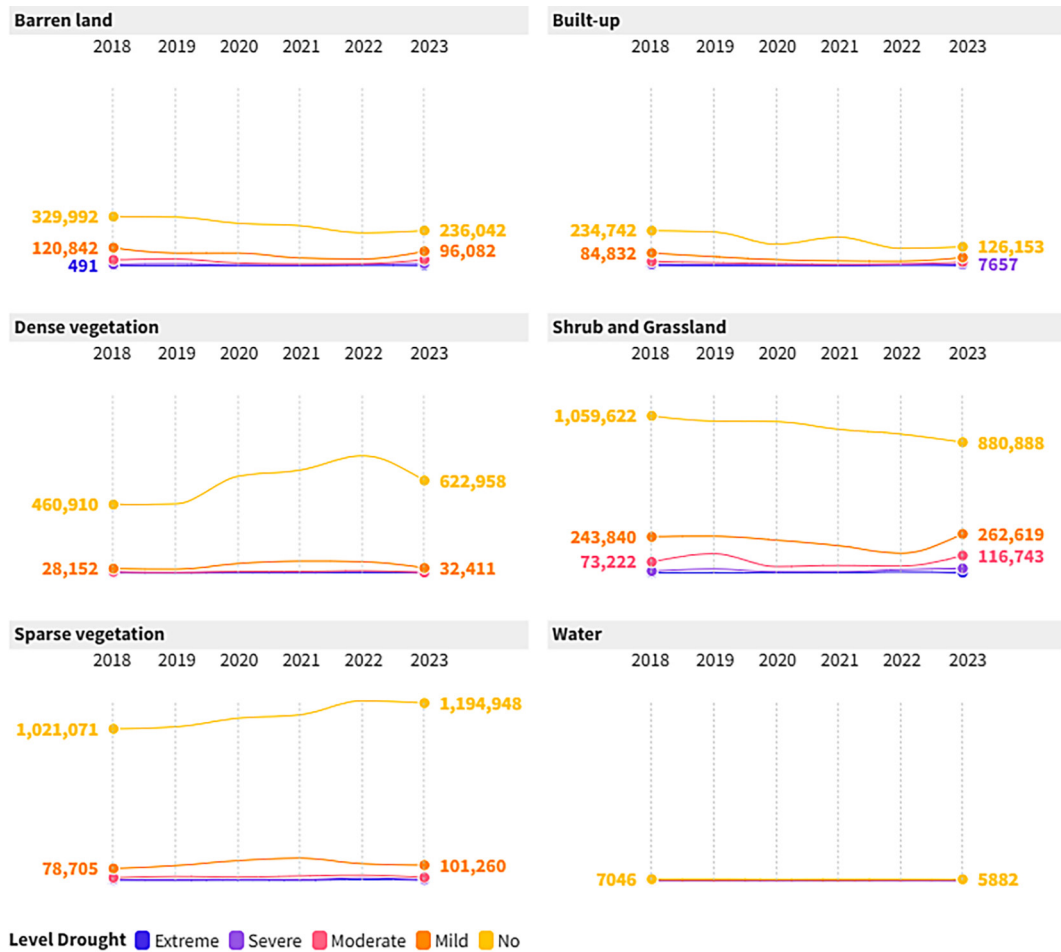


Figure 11. Land cover class exposed by drought in NTT Province, Republic of Indonesia in between 2018 and 2023

## CONCLUSIONS

The study was successfully conducted in the NTT Province based on the data from satellite remote sensing sourced from the Landsat-8 OLI/TIRS mission observed in 2018 to 2023. This study provided new insights into drought monitoring based on temporal changes in plants, especially in tropical regions. Three indices were created to see the drought exposure each year, namely TCI, VCI and VHI, where VHI was used as the main indicator for making drought classes. Then, the drought class was processed through analyzing the relationship between drought exposure and the temporal dynamic of land class obtained from NDVI classification.

Furthermore, the findings indicated high drought in the NTT Province due to seasonal dynamics, climate variability, seasonal farming, and fires, particularly in 2022 when there were land fires. This study found that seasonal farming and land fires were the factors causing high levels of drought in the NTT Province, which was not

revealed in previous studies. It is also important to remember that kind of land cover in the NTT Province has a great impact on drought. Field investigations was required to increase its accuracy and validation. As a result, this research can be utilized as a suitable reference for land and environmental planning in tropical regions, as well as for managing and reducing vulnerability from actual droughts. Last but not least, this research can be used as an evidence-based policy effort for the development of water resilience facilities by building dams in the areas in need, such as Sikka and Timor Tengah Selatan Sub-district, to meet community needs.

## REFERENCES

1. Abatzoglou, J.T., Dobrowski, S.Z., Parks, S.A., Hegewisch, K.C. 2018. TerraClimate, a high-resolution global dataset of monthly climate and climatic water balance from 1958–2015. *Scientific Data*, 5(1), 170191. <https://doi.org/10.1038/sdata.2017.191>

2. Akbar, T.A., Hassan, Q.K., Ishaq, S., Batool, M., Butt, H.J., Jabbar, H. 2019. Investigative spatial distribution and modelling of existing and future urban land changes and its impact on urbanization and economy. *Remote Sensing*, 11(2), 105. <https://doi.org/10.3390/rs11020105>
3. Al-Kindi, K.M., Al Nadhairi, R., Al Akhzami, S. 2023. Dynamic change in normalised vegetation index (ndvi) from 2015 to 2021 in dhofar, southern oman in response to the climate change. *Agriculture (Switzerland)*, 13(3). <https://doi.org/10.3390/agriculture13030592>
4. Almouctar, M.A.S., Wu, Y., Zhao, F., Qin, C. 2024. Drought analysis using normalized difference vegetation index and land surface temperature over Niamey region, the southwestern of the Niger between 2013 and 2019. *Journal of Hydrology: Regional Studies*, 52(August 2023), 101689. <https://doi.org/10.1016/j.ejrh.2024.101689>
5. BPS-Statistics Nusa Tenggara Timur Province, 2024a. Drought Victims (People), 2018–2020. URL <https://ntt.bps.go.id/indicator/27/913/2/korban-kekeringan.html> (accessed 6.13.24).
6. BPS-Statistics Nusa Tenggara Timur Province, 2024b. Drought Victims (People), 2021–2023. URL <https://ntt.bps.go.id/indicator/27/913/1/korban-kekeringan.html> (accessed 6.13.24).
7. BPS-Statistics Nusa Tenggara Timur Province, 2024c. Nusa Tenggara Timur Province in Figures. URL <https://ntt.bps.go.id/publication/2024/02/28/56eb9d4253a9d35283615899/provinsi-nusa-tenggara-timur-dalam-angka-2024.html> (accessed 7.23.24).
8. Bureau of Meteorology Australia, 2024. Indian Ocean influences on Australian climate. URL <http://www.bom.gov.au/climate/iod/> (accessed 7.30.24).
9. Copernicus Climate Change Service (C3S), 2017. ERA5: Fifth generation of ECMWF atmospheric re-analyses of the global climate. URL <https://cds.climate.copernicus.eu/cdsapp#!/home> (accessed 7.20.24).
10. Dai, A., Zhao, T., Chen, J. 2018. Climate change and drought: a precipitation and evaporation perspective. *Current Climate Change Reports*, 4(3), 301–312. <https://doi.org/10.1007/s40641-018-0101-6>
11. Diem, P.K., Pimple, U., Sitthi, A., Varnakovida, P., Tanaka, K., Pungkul, S., Leadprathom, K., LeClerc, M.Y., Chidthaisong, A. 2018. Shifts in growing season of tropical deciduous forests as driven by El Niño and La Niña during 2001–2016. *Forests*, 9(8), 448. <https://doi.org/10.3390/f9080448>
12. Ermida, S.L., Soares, P., Mantas, V., Göttsche, F.-M., Trigo, I.F. 2020. Google earth engine open-source code for land surface temperature estimation from the landsat series. *Remote Sensing*, 12(9), 1471. <https://doi.org/10.3390/rs12091471>
13. Ghebregabher, M.G., Yang, T., Yang, X., Eyassu Sereke, T. 2020. Assessment of NDVI variations in responses to climate change in the Horn of Africa. *Egyptian Journal of Remote Sensing and Space Science*, 23(3), 249–261. <https://doi.org/10.1016/j.ejrs.2020.08.003>
14. Karuniasa, M., Pambudi, P.A. 2022. The analysis of the El Niño phenomenon in the East Nusa Tenggara Province, Indonesia. *Journal of Water and Land Development*, 180–185. <https://doi.org/10.24425/jwld.2022.140388>
15. Kennedy, P.S.J. 2023. The problem of food security in the indonesia border area of Nusa Tenggara Timur Province with Timor Leste Country. *KnE Social Sciences*, 2023, 167–177. <https://doi.org/10.18502/kss.v8i9.13329>
16. Li, J., Wu, C., Xia, C.-A., Yeh, P. J.-F., Hu, B.X., Huang, G. 2021. Assessing the responses of hydrological drought to meteorological drought in the Huai River Basin, China. *Theoretical and Applied Climatology*, 144(3–4), 1043–1057. <https://doi.org/10.1007/s00704-021-03567-3>
17. Liu, Y., Zhu, Y., Ren, L., Singh, V.P., Yong, B., Jiang, S., Yuan, F., Yang, X. 2019. Understanding the spatiotemporal links between meteorological and hydrological droughts from a three-dimensional perspective. *Journal of Geophysical Research: Atmospheres*, 124(6), 3090–3109. <https://doi.org/10.1029/2018JD028947>
18. NOAA, 2024. Cold & Warm Episodes by Season. URL [https://origin.cpc.ncep.noaa.gov/products/analysis\\_monitoring/ensostuff/ONI\\_v5.php](https://origin.cpc.ncep.noaa.gov/products/analysis_monitoring/ensostuff/ONI_v5.php) (accessed 7.30.24).
19. Nopia, S., Fauzi, A.I., Sakti, A.D., Nuha, M.U., Anika, N., Putra, R., Siregar, D.I., Prasetyo, B.A., Julzarika, A., Wikantika, K. 2023. Drought analysis in Indonesia’s rice fields due to the 2015 El Nino using standardized precipitation index (SPI). 050014. <https://doi.org/10.1063/5.0115095>
20. Ogashawara, I., Bastos, V. 2012. A Quantitative approach for analyzing the relationship between urban heat islands and land cover. *Remote Sensing*, 4(11), 3596–3618. <https://doi.org/10.3390/rs4113596>
21. Pouyan, S., Bordbar, M., Ravichandran, V., Tiefenbacher, J.P., Kherad, M., Pourghasemi, H.R. 2023. Spatiotemporal monitoring of droughts in Iran using remote-sensing indices. *Natural Hazards*, 117(1), 1–24. <https://doi.org/10.1007/s11069-023-05847-9>
22. Putri, R.F., Rokhim, A.A., Prakosa, M.G., Hastari, N.R.F., Adhesti, Y.M.P., Junaedi, R.N., Ramdani, H.P., Omar, R.C. 2021. Analysis of Land Resources Balance in Nusa Tenggara Timur Province. *IOP Conference Series: Earth and Environmental Science*, 686(1), 012006. <https://doi.org/10.1088/1755-1315/686/1/012006>
23. Stanke, C., Kerac, M., Prudhomme, C., Medlock, J., Murray, V. 2013. Health effects of drought: a

- systematic review of the evidence. *PLoS Currents*. <https://doi.org/10.1371/currents.dis.7a2cee9e980f91ad7697b570bcc4b004>
24. U.S. Geological Survey. 2020. USGS EROS Archive - Landsat Archives - Landsat 8-9 OLI/TIRS Collection 2 Level-2 Science Products. <https://doi.org/10.5066/P9OGBGM6>
  25. Wang, P., Li, X., Tang, J., Yang, J., Ma, Y., Wu, D., Huo, Z. 2023. Determining the critical threshold of meteorological heat damage to tea plants based on MODIS LST products for tea planting areas in China. *Ecological Informatics*, 77(July), 102235. <https://doi.org/10.1016/j.ecoinf.2023.102235>
  26. Welianto, A., 2023. Kebakaran di Pulau Palue Sikka, Lumbung Pangan Ludes hingga Api Merambat ke Permukiman. *TribunFlores.com*. URL <https://flores.tribunnews.com/2023/09/12/kebakaran-di-pulau-palue-sikka-lumbung-pangan-ludes-hingga-api-merambat-ke-permukiman> (accessed 7.30.24).
  27. Welianto, A., 2022. Warga Kota Maumere Panik, 10 Hektar Lahan di Waioti Sikka Ludes Terbakar. *TribunMaumere.com*. URL <https://flores.tribunnews.com/2022/11/01/warga-kota-maumere-panik-10-hektar-lahan-di-waioti-sikka-ludes-terbakar> (accessed 7.30.24).
  28. Zaki, M.K., Noda, K. 2022. A systematic review of drought indices in tropical Southeast Asia. *Atmosphere*, 13(5), 833. <https://doi.org/10.3390/atmos13050833>
  29. Zeng, J., Zhang, R., Qu, Y., Bento, V. A., Zhou, T., Lin, Y., Wu, X., Qi, J., Shui, W., Wang, Q. 2022. Improving the drought monitoring capability of VHI at the global scale via ensemble indices for various vegetation types from 2001 to 2018. *Weather and Climate Extremes*, 35(December 2020), 100412. <https://doi.org/10.1016/j.wace.2022.100412>
  30. Zeng, J., Zhou, T., Qu, Y., Bento, V.A., Qi, J., Xu, Y., Li, Y., Wang, Q. 2023. An improved global vegetation health index dataset in detecting vegetation drought. *Scientific Data*, 10(1), 338. <https://doi.org/10.1038/s41597-023-02255-3>
  31. Zeri, M., Williams, K., Cunha, A.P.M.A., Cunha-Zeri, G., Vianna, M.S., Blyth, E.M., Marthews, T.R., Hayman, G.D., Costa, J.M., Marengo, J.A., Alvalá, R.C.S., Moraes, O.L.L., Galdos, M.V. 2021. Importance of including soil moisture in drought monitoring over the Brazilian semiarid region: An evaluation using the JULES model, in situ observations, and remote sensing. *Climate Resilience and Sustainability*, April, 1–18. <https://doi.org/10.1002/cli2.7>